anion in the solid lattice may also be a limiting factor in this situation, but it is evident that the effect of the thiocyanate ion added as part of the catalyst is insignificant compared to the effect of the acidic ion.

The loss of a bidentate ligand and its replacement by two monodentate anions would normally be expected to produce a *cis*-diacido complex. Such complexes are produced by the deamination of $[Cr(en)_3]Cl_3$ and $[Cr(pn)_3]Cl_3$, but the corresponding thiocyanate complexes yield *trans*-dithiocyanato products.[1] The *trans* effect in substitution reactions in square-planar complexes is well known and there have been several attempts to explain substitution in octahedral complexes by the *trans* effect.[12,13] Recently, an infrared study of nitrosylruthenium complexes showed a *trans*-directing influence of several ligands based on the Ru–NO stretching frequency. It was further shown that the *cis* effect was smaller than the *trans* effect, although too large to ignore.[14] Although these studies have dealt with other metals, they may have some validity for chromium(III) systems. Recently, evidence was reported for a *trans* effect in a chromium(III) reaction.[15]

(12) F. Basolo and R. G. Pearson, *Progr. Inorg. Chem.*, **4**, 381 (1963), and references therein.
(13) F. Basolo and R. G. Pearson, "Mechanisms of Inorganic Reactions," 2nd ed, John Wiley & Sons, Inc., New York, N. Y., 1967, Chapter 5 and references therein.
(14) E. E. Mercer, W. A. McAllister, and J. R. Durig, *Inorg. Chem.*, **5**, 1881 (1966).
(15) P. Moore, F. Basolo, and R. G. Pearson, *ibid.*, **5**, 223 (1966).

The rate of deamination depends upon the rate at which metal–ligand bonds are broken and may involve electrophilic attack by the protonated amine catalyst; on the other hand, the protonation of the ligand could be subsequent to the breaking of a metal–ligand bond. First-order dependence on the acidic species present indicates that electrophilic attack is involved in the rate-determining step. This accounts for the activation energy of the catalyzed reactions being lower than those of the uncatalyzed reactions where the metal–ligand bond must be broken without the aid of protonation. A thiocyanate ion entering the coordination site vacated by the breaking loose of a protonated end of an ethylenediamine molecule might then exert a strong enough *trans* effect on the position *trans* to it that another ethylenediamine molecule has one end loosened. This would lead to a *trans* product. If the chloride ion exerts a strong *cis* effect or does not exert a strong *trans* effect, the bound end of the protonated ethylenediamine molecule may break loose and the second chloride enter there. This would give a *cis* product.

It is impossible at this time to assess the relative importance of these effects as they apply to the reactions studied here. It is also quite possible that these effects assume different proportions in solid-state reactions than in solution reactions. Structural isomerism of the products can be predicted by the assumption of either a strong *trans* effect by NCS^- or a strong *cis* effect by Cl^-.

Electrochemical and Spectral Studies of Dimeric Iron(III) Complexes[1]

Harvey J. Schugar, A. T. Hubbard, F. C. Anson, and Harry B. Gray[2]

Contribution No. 3643 from the Gates and Crellin Laboratories of Chemistry, California Institute of Technology, Pasadena, California 91109.
Received January 29, 1968

Abstract: The electrochemical behavior of the monomeric ($EDTA\text{-}Fe^{III}OH^{2-}$) and dimeric ($(EDTA\text{-}Fe^{III})_2O^{4-}$) complexes present at equilibrium in the Fe^{III}–EDTA system at pH 9 has been characterized. Fast-sweep cyclic voltammetry in pH 9 buffered media reveals two reduction waves and a single anodic wave. Both the monomer and dimer, by a two-electron reduction, are reduced to ferrous monomer. In buffered media, slow-sweep linear voltammetry with thin-layer electrodes produces single cathodic and anodic waves because the dimer dissociates as the monomer is reduced. The rate constant for dissociation of dimer is estimated at 0.5 sec^{-1} from chronocoulometric measurements. A pathway involving solvent assistance is suggested as the mechanism of dimer breakup.

The formation, hydrolysis, and dimerization of ferric complexes of ethylenediaminetetraacetate (EDTA) and related aminocarboxylic acids have received considerable attention. A comprehensive study of the latter two phenomena with references to prior work has been reported by Gustafson and Martell.[3] They have shown that the ferric complexes of EDTA, N-hydroxyethylethylenediaminetriacetate (HEDTA), cyclohexanediaminetetraacetate (CDTA), and nitrilotriacetate (NTA) are hydrolyzed by alkali to give equilibrium mixtures of monohydroxy monomers and binuclear complexes; in a subsequent step, dihydroxo mononuclear complexes are formed. The observed magnetic and spectral properties of the dimer in the $HEDTA\text{-}Fe^{III}$ system led us to formulate its structure as containing an approximately linear Fe–O–Fe bridging unit.[4] The proposed Fe–O–Fe bridging unit in the dimer has been verified by an X-ray structural determination of the salt $[enH_2^{2+}][(HEDTA\text{-}Fe^{III})_2O]\cdot 6H_2O$, where enH_2^{2+} is

(1) This research was supported by the National Science Foundation.
(2) Author to whom correspondence should be addressed.
(3) R. L. Gustafson and A. E. Martell, *J. Phys. Chem.*, **67**, 576 (1963).

(4) H. Schugar, C. Walling, R. B. Jones, and H. B. Gray, *J. Am. Chem. Soc.*, **89**, 3712 (1967).

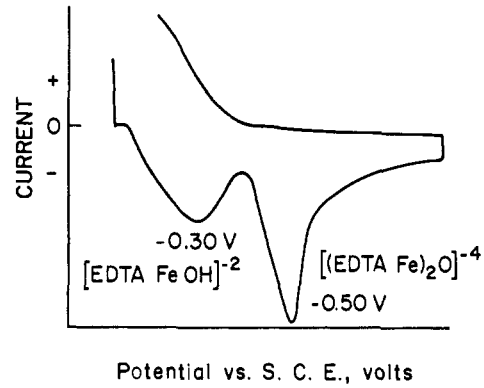

Figure 1. Current–potential curve for 10 m*F* EDTA-Fe^{III} in 1.0 *F* $NaClO_4$ supporting electrolyte, buffered at pH 9.0 with 50 m*F* EDTA: hanging drop mercury electrode, sweep rate = 25 V/sec. Anodic currents are shown as positive.

ethylenediammonium.[5] The crystalline dimers isolated with EDTA as the ligand are thought to have the analogous structure (EDTA-Fe^{III})$_2O^{4-}$ because these materials exhibit infrared absorption at ~830 cm^{-1} that is characteristic of the Fe–O–Fe unit; in addition, the visible spectra of (EDTA-Fe^{III})$_2O^{4-}$ and (HEDTA-Fe^{III})$_2O^{2-}$ are virtually identical.[4] Kolthoff and Auerbach have studied the EDTA-Fe^{III} system polarographically over the pH range 1–11.[6] In alkaline solutions where the dimer is present,[3] single waves characteristic of a reversible one-electron reduction were observed, along with a slight (~5%) decrease in the cathodic diffusion current constant. Spectral analysis of these solutions, which had a faint orange color, revealed large deviations from Beer's law.

This paper presents detailed electrochemical and electronic spectral studies of the equilibrium between EDTA-$Fe^{III}OH^{2-}$ and (EDTA-Fe^{III})$_2O^{4-}$. It was undertaken both to further define structural and dynamical aspects of this system and to develop an electrochemical method for the study of binuclear complex formation in related chemical systems.

Experimental Procedures

Solutions were prepared with triply distilled water, the second distillation being from $KMnO_4$. The salt $NaFe^{III}EDTA \cdot 3H_2O$ was prepared by treating $Fe(OH)_3$ with a stoichiometric amount of the monosodium salt of EDTA at 80–90° for several minutes. Slow evaporation of the resulting yellow solution produced well-formed brown crystals. Anhydrous $NaClO_4$ was obtained from the G. F. Smith Chemical Co.; the other salts and the EDTA used were reagent-grade materials. The monomer–dimer mixtures at pH 9 were prepared by adding appropriate amounts of Na_4(EDTA-Fe^{III})$_2O \cdot 12H_2O$[4] to solutions already buffered at pH 9. A Leeds and Northrup Model 7401 pH meter equipped with extension calomel and glass electrodes, and regularly calibrated with standard buffers, was used for pH measurements. Short-range pH paper gave equivalent results.

Spectra were measured on a Cary Model 14 recording spectrophotometer, generally using 1.0-cm matched cells or a 1.0-cm cell containing a removable solid silica spacer that gave a path length of 0.005 cm. A cylindrical cell with a 5.0-cm path length was used to measure the visible solution spectra of solutions that contained less than 0.001 *F* Fe^{III}-EDTA. The optical densities were corrected for blank absorption. The supporting electrolytes used for the spectral measurements gave negligible blank absorptions.

Previously described micrometer-type, thin-layer electrodes[7] and associated electronics[8] were used for the slow linear-sweep voltammetry. The current–potential curves were recorded with an X–Y recorder. Oxygen was removed from solutions with water-saturated N_2 that was prescrubbed with solutions of vanadous and chromous ions. The entire electrode assembly was enclosed in a glove bag which was continuously swept with nitrogen.

The cyclic voltammetry and chronocoulometry were carried out with apparatus similar to that which has been previously described.[9] A standard three-compartment cell was used with the test solution present in each compartment. The central compartment (which contained the mercury working electrode) was deoxygenated by sparging with prepurified nitrogen that was also passed over hot Cu turnings at 350° to remove any residual O_2. The auxiliary and reference electrodes were in separate cell compartments that were connected to the central compartment by glass frits. A commercially available hanging mercury drop electrode was used (Brinkman Instruments, Inc.); the area of each drop was 0.032 cm^2. Potential sweep rates from *ca.* 1 to 25 V/sec were employed.

The solutions contained 0.3 to 10.0 m*F* Fe^{III}-EDTA, 1.0 *F* $NaClO_4$ as supporting electrolyte, and 0.05 *F* EDTA to provide buffering action at pH 5.3 or 9.0. Blank corrections for the currents and charge were made by repeating the experiments in buffered supporting electrolyte.

The potential-step chronocoulometric experiments followed standard practice.[10] The initial and final potentials were carefully chosen to avoid oxidation of the electrode and to assure diffusion control of the faradaic reaction. At pH 5, the measured charge, after correction for double-layer charging, was identical for final potentials between −0.30 and −0.50 V *vs.* sce for EDTA-$Fe^{III}OH_2^-$. However, at pH 9.0, the choice of the final potential was more difficult since the respective peak potentials for EDTA-$Fe^{III}OH^{2-}$ and its dimer were about −0.30 and −0.50 V. The data indicated that a final potential of −0.35 V was sufficiently large to reduce the monomer without significant reduction of the dimer. This choice was supported by the good agreement between the charge measured for monomer reduction at very short times and the diffusion-limited charge expected from the known distribution of iron in the equilibrium mixture.

The cyclic voltammograms and chronocoulograms were recorded with a Tektronix Model 564 storage oscilloscope. Data were read directly from photographs of the traces.

Results

Cyclic Voltammetry. The characteristics of the monomer–dimer equilibrium in the Fe^{III}-EDTA system at pH 9 are readily established with this technique. A typical current–potential curve is shown in Figure 1 for a high sweep rate (25 V/sec). Two cathodic waves are observed. The dependence of the relative sizes of these waves on the total iron chelate concentration is diagnostic of a monomer–dimer equilibrium. Namely, as the chelate concentration increases at constant pH, the peak current of the second wave is found to increase significantly relative to that of the first wave. The fact that only one anodic wave is evident suggests that both the ferric dimer and monomer are reduced to a ferrous monomer.[11]

With repetitive sweeps, the second cathodic wave diminishes and almost disappears. This suggests that the establishment of the monomer–dimer equilibrium from the ferric monomer generated on each anodic cycle is relatively slow and supports the suggestion that ferrous monomer is the sole reduction product. Once

(5) S. J. Lippard, H. J. Schugar, and C. Walling, *Inorg. Chem.*, **6**, 1825 (1967).

(6) I. M. Kolthoff and C. Auerbach, *J. Am. Chem. Soc.*, **74**, 1452 (1952).

(7) A. T. Hubbard and F. C. Anson, *Anal. Chem.*, **36**, 723 (1964).

(8) A. T. Hubbard and F. C. Anson, *ibid.*, **38**, 58 (1966).

(9) F. C. Anson and D. A. Payne, *J. Electroanal. Chem.*, **13**, 35 (1967).

(10) R. A. Osteryoung and F. C. Anson, *Anal. Chem.*, **36**, 975 (1964).

(11) Qualitatively similar results were observed when excess EDTA was omitted and 0.5 *M* Na_2HPO_4 was used as a combination buffer–(supporting electrolyte). However, a distinctly lighter orange-red coloration of these solutions suggested competitive complex formation with the HPO_4^{2-}, and this approach was abandoned. In addition, the HEDTA-Fe^{III} system was studied in a preliminary way. Two cathodic waves and a single anodic wave were observed; the relative heights of the cathodic waves have the concentration dependence mentioned above.

the cathodic sweep rate is made great enough to "freeze" the equilibrium, the ratio of the two cathodic peak currents should be independent of the sweep rate. This is the observed behavior. The other extreme, illustrated in the latter part of this paper, occurs at low sweep rates where the complete dissociation of the dimer has time to take place and a single cathodic wave results.

According to the scheme formulated above, the second cathodic wave corresponds to the reduction of the dimer and should, therefore, represent a two-electron reduction. To test this point, the peak current was analyzed as a function of sweep rate by means of the Randles–Sěvčik′ equation[12,13]

$$i_p = 2.69 \times 10^5 n^{3/2} A D^{1/2} C V^{1/2}$$

where i_p = peak current, A = electrode area, V = sweep rate, V/sec, C = concentration of electroactive species, D = diffusion coefficient, n = number of electrons involved in the electrochemical change. If D is assumed to be the same for Fe^{III}-EDTA$^-$, Fe^{III}-EDTA(OH)$^{2-}$, and the ferric dimer, the ratio of the peak current, $(i_p)_m$, observed at pH 5.3 for the Fe^{III}-EDTA$^-$ to the peak current, $(i_p)_d$, observed for the second wave at pH 9.0 which corresponds to the dimer, should be given by

$$\frac{(i_p)_m/V^{1/2}}{(i_p)_d/V^{1/2}} = \frac{(n^{3/2})_m C_m}{(n^{3/2})_d C_d} = \frac{C_m}{C_d}\frac{1}{(n^{3/2})_d}$$

where C_m and C_d are the monomer and dimer concentrations, respectively.

Two sets of experiments were conducted with total Fe(III) concentrations of 0.01 and 0.006 F. At pH 5.3, Fe^{III}-EDTA$^-$ was the only complex present (see the pK values for hydrolysis below) and the concentration of this monomeric species was therefore 0.01 or 0.006 F. However, the dimer concentrations must be independently known. The appropriate equilibria are listed below.

$$\text{EDTA-Fe}^{III}(OH_2)^- \rightleftharpoons \text{EDTA-Fe}^{III}OH^{2-} + H^+$$

$$K_1 = \frac{[\text{EDTA-Fe}^{III}OH^{2-}][H^+]}{[\text{EDTA-Fe}^{III}(OH_2)^-]}$$

$$\text{EDTA-Fe}^{III}OH^{2-} \rightleftharpoons \text{EDTA-Fe}^{III}(OH)_2{}^{3-} + H^+$$

$$K_2 = \frac{[\text{EDTA-Fe}^{III}(OH)_2{}^{3-}][H^+]}{[\text{EDTA-Fe}^{III}OH^{2-}]}$$

$$2\text{EDTA-Fe}^{III}OH^{2-} \rightleftharpoons (\text{EDTA-Fe}^{III})_2O^{4-}$$

$$K_d = \frac{[(\text{EDTA-Fe}^{III})_2O^{4-}]}{\text{EDTA-Fe}^{III}(OH)^{2-}]^2}$$

Straightforward algebraic manipulation of these equilibria along with a mass balance produces the quadratic equation $4E^2 - E(4C + a^2/K_d) + C^2 = 0$ where E is the dimer concentration, a is $(1 + [H^+]/K_1 + K_2/[H^+])$, and C is the total formality of iron present. Selecting the published values of pK_1 = 7.58[3] and pK_2 = 9.41[14] results in an a of 1.427 at pH 9.0. Gustafson and Martell found pK_d to be −2.95 (25°, 1.0 F KCl). By trial and error, we find it necessary to assume that pK_d ≅ −2.53 in order to obtain a Beer's law plot (26°, 1.0 F $NaClO_4$, 0.05 F EDTA buffer, pH 9.0). Figure 2 illustrates the linear relationship between the optical density at 540 mμ (see discussion in the next paragraph) and the dimer concentration calculated from the above quadratic equation. The slope of the line in Figure 2 fixes the molar extinction coefficient at ~115, which compares favorably with the value of ~121 determined for the (HEDTA-Fe^{III})$_2O^{2-}$ dimer.[4]

(12) J. E. B. Randles, *Trans. Faraday Soc.*, **44**, 327 (1948).
(13) A. Sěvčik′, *Collection Czech. Chem. Commun.*, **13**, 349 (1948).
(14) G. Schwarzenbach and J. Heller, *Helv. Chim. Acta*, **34**, 576 (1951).

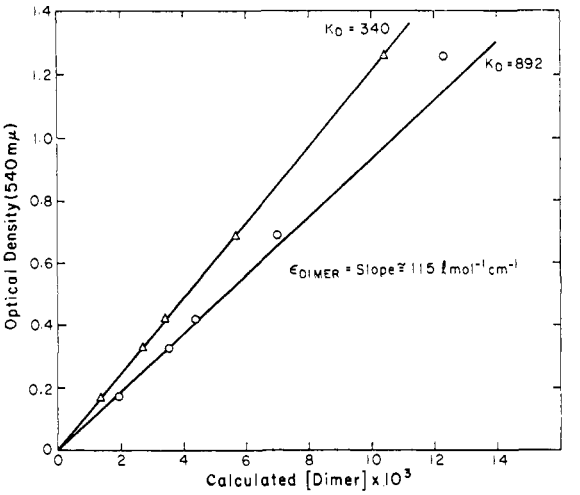

Figure 2. Beer's law plot for monomer–dimer equilibrium at 26° in 1.0 F $NaClO_4$ with 0.05 F EDTA as buffer; K_D = 892 obtained by Gustafson and Martell[3] at 25° in 1.0 F KCl without EDTA buffer.

The complete ultraviolet and visible solution spectra of Fe^{III}-EDTA$^-$ and the equilibrium mixture of EDTA-$Fe^{III}OH^{2-}$ and dimer are shown in Figures 3 and 4, respectively. Since EDTA-$Fe^{III}(OH_2)^-$, HEDTA-$Fe^{III}(OH_2)$, and HEDTA-$Fe^{III}(OH)_2{}^{2-}$ do not absorb light at 540 mμ, the absorption of EDTA-$Fe^{III}OH^{2-}$ is assumed to be zero there also. This is consistent with the observed Beer's law behavior.

Several independent measurements of i_p *vs.* $V^{1/2}$ were carried out using sweep rates great enough to ensure that the monomer–dimer equilibrium was effectively "frozen" (>2.5 V/sec). These yielded linear plots with intercepts at the origin for both the single Fe^{III}-EDTA$^-$ wave at pH 5.3 and the second of the two waves observed at pH 9.0. Values of $(i_p)_m/V^{1/2}$ and $(i_p)_d/V^{1/2}$ were calculated from the slopes of the plots. When these values and the known Fe^{III}-EDTA$^-$ and calculated dimer concentrations were substituted into the equation, values of n_d ranging from 2.0 to 2.2 were obtained, thus confirming that the second wave corresponds to the dimer.

Thin-Layer Voltammetry. Slow linear-sweep voltammetry with a platinum electrode thin layer cell was also employed to study monomer–dimer equilibrium mixtures. The resulting data are summarized in Table I. For solutions buffered at pH 9.0, with $HPO_4{}^{2-}$–$PO_4{}^{3-}$, $HCO_3{}^-$–$CO_3{}^{2-}$, or excess EDTA, single cathodic and anodic waves are observed (Figure 5). The waves are generally centered at about −0.24 V (*vs.* sce), the cathodic peak appearing at about −0.30 V and the anodic peak at about −0.20 V. Apparently, the monomer–dimer equilibrium is maintained during the relatively long time (several minutes) required for the cathodic sweep with the thin layer cell. In effect, all the iron(III) is reduced *via* monomeric Fe^{III}-EDTA$^-$. Coulometric studies verified that the single cathodic wave corresponds to the total amount of iron in the cell.

The measured average peak potential in pH 9 media buffered with 50 mF EDTA is about −0.24 V. This system is uncomplicated by competing coordination by

Table I. Peak Potentials Obtained with Slow Linear-Sweep Voltammetry with a Thin Layer Cell[a]

Buffer composition	pH	Supporting electrolyte	$E_{cathodic}$, V	E_{anodic}, V	E_{av}, V
0.635 F $NaHCO_3$	9	1.0 F $NaHCO_3/CO_3$	−0.29	−0.19	−0.24
+ 0.182 F Na_2CO_3			−0.32	−0.22	−0.27
0.050 F EDTA	9	1.0 F $NaClO_4$	−0.27	−0.21	−0.24[b]
1.0 F Na_2HPO_4	9	1.0 F Na_2HPO_4	−0.30	−0.20	−0.25

[a] Total Fe(III) = 3 mF, 1-μl cell volume, sce reference electrode. [b] Total charge calculated from Faraday's law = $3 \times 10^{-3} \times 10^{-6} \times 96{,}489 = 289$ μC. Experimentally, charge = 290 ± 15 μC.

anions such as HPO_4^{2-}, CO_3^{2-}, and HCO_3^-. A theoretical value for the reversible peak potential of −0.21 V was calculated in the following way.

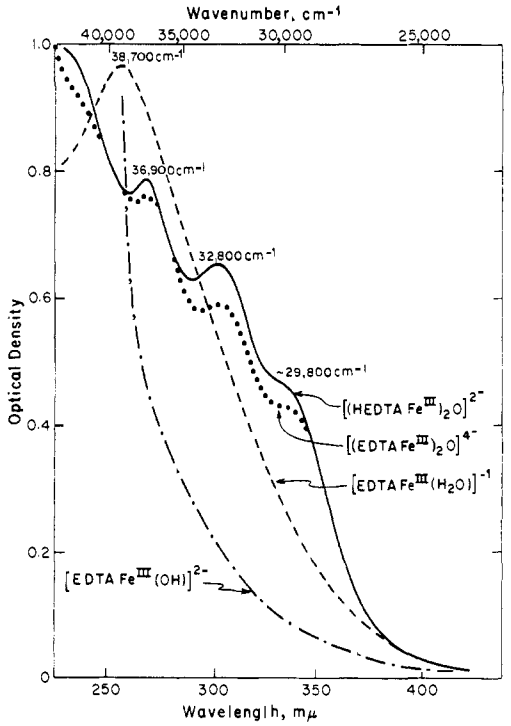

Figure 3. Ultraviolet absorption spectra: 20 mF EDTA-Fe^{III} at pH 5.3, 1.0 F $NaClO_4$, 0.05 F EDTA, 0.005 cm (- - - -); 20 mF EDTA-Fe^{III} at pH 9.0, 1.0 F $NaClO_4$, 0.05 F EDTA, 0.005 cm (· · · ·); 19 mF HEDTA-Fe^{III} at pH 7.5, 1.0 F $NaClO_4$, 0.05 F HEDTA, 0.005 cm (———); 0.5×10^{-4} mF EDTA-Fe^{III} at pH 9.0, 1.0 F $NaClO_4$, 0.05 F EDTA, 1.0 cm, distributed 100% as monomer (- · - ·); all measurements at 26°.

In alkaline media the redox potential is affected by the equilibria of the ferric complexes previously described and the protolytic equilibria of the ferrous complexes listed below.

$$EDTA\text{-}Fe^{II\,2-} \rightleftharpoons EDTA\text{-}Fe^{II}(OH)^{3-} + H^+ \quad pK_1' = 9.07^{14}$$

$$EDTA\text{-}Fe^{II}(OH)^{3-} \rightleftharpoons EDTA\text{-}Fe^{II}(OH)_2^{4-} + H^+ \quad pK_2' = 9.84^{14}$$

There are two additional equations describing material balances.

$$C = [EDTA\text{-}Fe^{III-}] + [EDTA\text{-}Fe^{III}(OH)^{2-}] + [EDTA\text{-}Fe^{III}(OH)_2^{3-}] + 2[(EDTA\text{-}Fe^{III})_2O^{4-}]$$

$$C' = [EDTA\text{-}Fe^{II\,2-}] + [EDTA\text{-}Fe^{II}(OH)^{3-}] + [EDTA\text{-}Fe^{II}(OH)_2^{4-}]$$

When expressions relating $[EDTA\text{-}Fe^{III-}]$ and $[EDTA\text{-}Fe^{III\,2-}]$ to C and C' (and appropriate equilibrium constants) are substituted in the known relationship $E = -0.13 + 0.059 \log [EDTA\text{-}Fe^{III-}]/[EDTA\text{-}Fe^{II\,2-}]$, the following equation results.

$$E = -0.13 + 0.059 \log \frac{C}{C'} + 0.059 \log ([H^+]^2 + K_1'[H^+] + K_1'K_2') - 0.059 \log ([H^+]^2 + K_1[H^+] + K_1K_2) + 2K_dK_1^2[EDTA\text{-}Fe^{III-}]$$

Assuming that C and C' are equal at the peak cathodic current, $E = 0.21$ V at pH 9.0 for a solution 3 mF in iron (*e.g.*, C and C' are 1.5 mF at the peak current). At this concentration, the calculated change in potential results chiefly from the hydrolysis reactions. For example, the $2K_dK_1^2[EDTA\text{-}Fe^{III-}]$ term drops out when dimerization is neglected, and the potential is calculated to be reduced by −0.075 V instead of −0.082 V. At higher concentrations, the effects of dimer formation on the potential become more important. When C increases from 1.5 to 30 mF the perturbation from dimer formation increases from 0.007 to 0.024 V. Under favorable circumstances, such a concentration dependency of the redox potential could be observed.

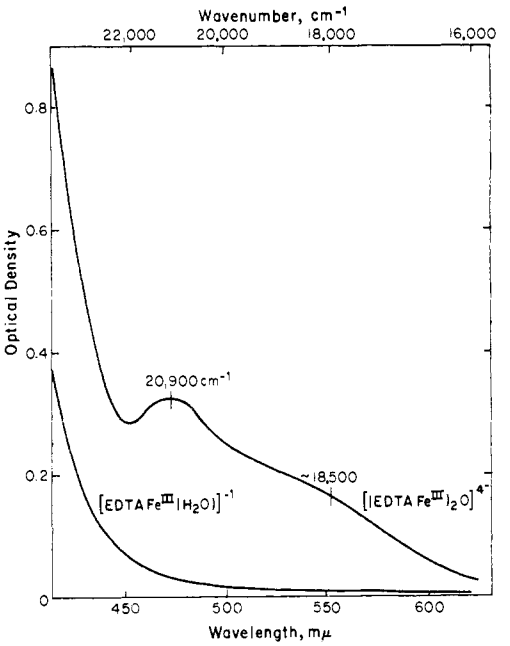

Figure 4. Visible absorption spectra: 20 mF EDTA-Fe^{III} at pH 5.3 (lower curve) and same at pH 9.0, 0.2 cm, 26°, 1.0 F $NaClO_4$, 0.05 F EDTA.

Rate Constants for the Dimer–Monomer Equilibrium. The rate constants for this equilibrium were calculated

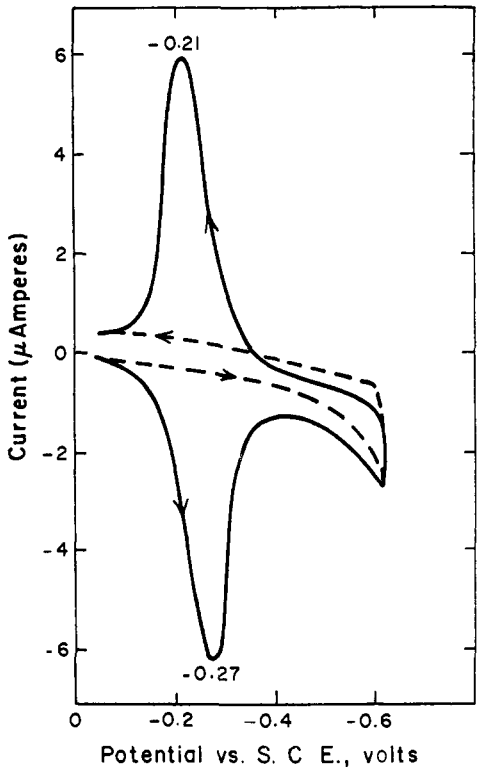

Figure 5. Current–potential curve for 1 μl of 3 m*F* EDTA-Fe^{III} solution with thin-layer electrode. Supporting electrolyte was 1.0 *F* $NaClO_4$–0.05 *F* EDTA adjusted to pH 9 with NaOH. The potential sweep rate was 2.0 mV/sec. The electrode was prewashed with a 1 m*F* KI solution (A. T. Hubbard and F. C. Anson, *Anal. Chem.*, **38**, 1601 (1966)) to reduce the magnitude of the residual current, shown with the dashed line. Anodic currents are shown as positive.

from the charge–time transients resulting from a series of potential step chronocoulometric experiments. Referring to Figure 1, only the monomeric ferric species will be directly reduced when the electrode potential is stepped from E_0 to −0.35 V *vs.* sce. However, dimer disappearance will commence as soon as the concentration of the ferric monomer at the electrode surface is lowered by the electroreduction. The chronocoulometric charge–time data are therefore influenced by the kinetics of the dimer dissociation. There are two limiting conditions corresponding to very long times or very short times. At short times, the equilibrium is essentially "frozen" because contributions from the dimer are eliminated and, at "long" times, all the Fe(III) species are reduced and the equilibrium is in effect invisible. These situations parallel those already described for rapid and slow linear sweep voltammetry.

Unfortunately, this kinetic situation leads to nonlinear differential equations that cannot be solved analytically. However, Feldberg[15] has obtained a numerical solution that relates the experimental parameters (charge and time) to k_f, the desired rate constant for dimer dissociation (Figure 6). The kinetic scheme involved is

$$Ox_{mono} + e \rightleftharpoons Red_{mono}$$

$$Ox_{dimer} \underset{k_b}{\overset{k_f}{\rightleftharpoons}} 2Ox_{mono}$$

(15) The working curve shown in Figure 6 was derived by S. Feldberg. Details will be published in "Electroanalytical Chemistry; A Series of Advances," Vol. 3, A. J. Bard, Ed., Marcel Dekker, Inc., New York, N. Y., in press.

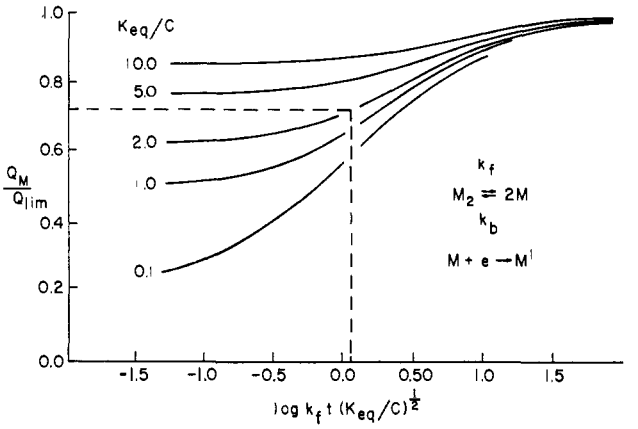

Figure 6. Computer-derived working curve for the electroreduction of a monomer which is in sluggish equilibrium with a dimer, according to Feldberg.[15]

where $k_f/k_b = [Ox_{mono}]^2/[Ox_{dimer}] = K_{eq}$. Other quantities used in Figure 6 are C, the total analytical concentration of Fe(III); Q_M, the faradaic charge measured at time t after the potential is stepped to −0.35 V *vs.* sce (Figure 1); and Q_{lim}, the theoretical diffusion limited value of Q_M that would result if all the iron were present as monomer.

In our experiments, C was held constant at 3 m*F* and Q_{lim} was approximated by chronocoulometry on a 3 m*F* solution of EDTA-Fe^{III}– at pH 5.3 (the potential was stepped from −0.08 to −0.30 V *vs.* sce). An inspection of Figure 6 shows that at short times and long times the slope of the family of curves (K_{eq}/C) is insensitive to the ratio Q_M/Q_{lim}; *i.e.*, the equilibrium is respectively "frozen" and "invisible." Procedurally, Q_M and Q_{lim} are measured at the same time t, corrected for double-layer charging, and their ratio is used to locate an intercept on the suitable K_{eq}/C curve which fixes a value of the x coordinate. The only unknown parameter is k_f.

For the above reaction scheme, Ox_{mono} must represent all the ferric monomers, since they are interconvertible by protolytic reactions that are much faster than the rate of dimer dissociation. With this rationale an "effective" equilibrium constant is constructed from the K_d determined by spectroscopic analysis: $K_{eq} = 1/\beta^2 K_d$, where β = EDTA-$Fe^{III}OH^{2-}/\Sigma Ox_{mono}$. For a 3 m*F* solution of EDTA-Fe^{III} at pH 9.0, a K_d of ~340 results in the iron being distributed as 38% dimer and the balance as ferric monomers. A material balance fixes β at 0.704. Therefore

$$K_{eq}/C = 1/C\beta^2 K_d = 2.0$$

Referring to Figure 6, the curve $K_{eq}/C = 2.0$ defines a Q_M/Q_{lim} of 0.60. This agrees satisfactorily with the above calculation that shows 62% of the iron is monomeric. The measured time dependency of Q_M/Q_{lim} is shown in Figure 7. At short times the "frozen" equilibrium is experimentally reflected in the limiting Q_M/Q_{lim} ratio of ~0.6. In the manner described above, k_f was found to be ~0.5 sec^{-1}.

Referring to Figure 6, the calculated value of k_f is sensitive to the value of K_{eq}/C. However, reasonable upper and lower limits can be established. For example if K_{eq}/C is ~4, the rather flat slope of that curve generates very large differences in the x ordinate for the range of Q_M/Q_{lim} values studied, and the calculated values of

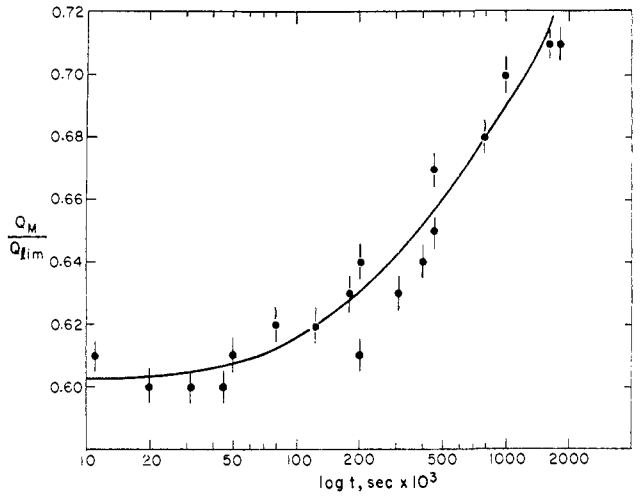

Figure 7. Time dependency of the ratio of the measured charge to the diffusion-limited charge.

k_f will vary over an unrealistically large range. If K_{eq}/C is as low as 0.50, then the calculated values of k_f at 0.5 and 1.0 sec would be about 2.4 sec^{-1} and would not drastically alter the value of k_f estimated above at $\sim$0.5 sec^{-1}. The estimated value seems plausible on additional grounds: if k_f is as small as 0.1 sec^{-1}, then it would be slow enough to measure with classical spectrophotometric techniques. This was not possible. If k_f is as large as 20 sec^{-1}, then the cathodic sweep rates used for the linear sweep voltammetry reported above would not have been fast enough for the ratio of the peak currents for the monomer and dimer to have been independent of sweep rate (*i.e.*, the Randles–Ševčik' equation would not have been obeyed). In fact, this ratio was observed to be constant with sweep rates from 2.5 to 22.5 V/sec.

Discussion

These electrochemical studies independently demonstrate the existence of a dimeric species in solution. This follows from the appearance of two cathodic waves, the dependence of their relative sizes on the total iron(III)–chelate concentration at constant pH, the marked collapse of the second cathodic wave with repetitive sweeps, and the fact that the wave assigned to the dimer represents a two-electron reduction. Also, the visible spectra of hydrolyzed Fe^{III}-EDTA solutions follow Beer's law when analyzed from the perspective of a monomer–dimer equilibrium. These findings verify the original discovery of dimer formation in this system by Gustafson and Martell.[3] The differing results obtained with the fast and slow potential sweep techniques also emphasize why dimer formation in labile systems can easily be missed[6] with relatively slow sweep techniques such as polarography. If the range of metal complex concentrations studied is too small or the dimerization constant is small, dimerization also will be hard to detect with any type of potentiometric measurement. In any event, in the classical study of the Fe^{III}-EDTA system by Schwarzenbach and Heller, neither potentiometry nor an analysis of the protolytic equilibria pointed to dimer formation in alkaline solutions.[14]

The similarity of the electronic spectra of the monomer–dimer equilibrium mixtures for both the Fe^{III}-EDTA and -HEDTA systems (Figure 3) suggests that the coordination is similar for both dimers. The structural determination of the HEDTA-containing dimer reveals the Fe–O–Fe bridging unit with pentadentate HEDTA attached to each metal, the hydroxyethyl group not being coordinated.[5] Oxo bridging in solution is supported by magnetic susceptibility data[4] and by preliminary laser-Raman studies that show the presence of the characteristic M–O–M stretching frequency at $\sim$830 cm^{-1}.[16] Also, equilibria between oxo- and significant amounts of dihydroxo-bridged species are considered improbable from the fast potential sweep studies in which only a single dimeric species is observed.

Whereas Gustafson and Martell did not propose a structure for $(EDTA\text{-}Fe^{III})_2O^{4-}$, they did suggest[3] that the analogous complex with HEDTA involves dihydroxo bridging or structures in which the hydroxyethyl groups participate, for example

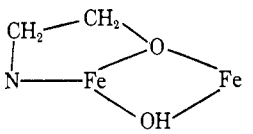

and

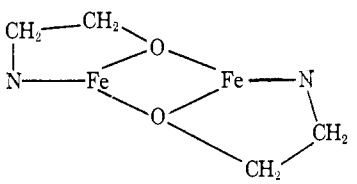

These structures were suggested partly because the chelate with HEDTA has a greater tendency to hydrolyze than the analogous chelate with EDTA, the respective pK values for formation of the monohydroxo complexes being 4.11 and 7.58. However, the similar electronic solution spectra and extinction coefficients of these dimers do not support the hypothesis that different bridging units are present. The best picture for the dimer containing EDTA is an oxo-bridged iron system containing two pentadentate EDTA groups, with one acetate group of each ligand not coordinated.

Pathway for Dimer Breakup

Finally, we turn to a consideration of the pathway for dimer breakup to monomer and the reverse association process. In view of the fact that the forward rate constant ($k \cong 0.5$ sec^{-1}) is as large as that measured[17,18] for the $[H^+]$-independent pathway for fragmentation of the postulated dihydroxo-bridged "aquo dimer"

(16) The fact that the solution magnetic moment of $(HEDTA\text{-}Fe^{III})_2O^{2-}$ is essentially the same as the 2.8 BM value measured at room temperature for a crystalline enH_2^{2+} salt suggests analogous structural features. The proximity of this magnetic moment to 2.88 BM coupled with the observation of similar Mössbauer spectra at 300 and 77°K led us to suggest[4] a spin-triplet ground state for these dimeric oxo-bridged complexes; a preliminary electronic structural analysis consistent with a spin-triplet ground state has been offered.[5] However, our more detailed magnetic susceptibility data at various temperatures down to 4.2°K show that the HEDTA and EDTA oxo-bridged complexes have diamagnetic ground states; thus the paramagnetism at room temperature is apparently due to the population of an excited electronic state. We are preparing a detailed account of these electronic structural properties (C. G. Barraclough, G. Rossman, H. Schugar, and H. B. Gray, to be published).

(17) H. Wendt, *Z. Elektrochem.*, **66**, 235 (1962).

(18) T. J. Conocchioli, E. J. Hamilton, Jr., and N. Sutin, *J. Am. Chem. Soc.*, **87**, 926 (1965).

$((H_2O)_4FeOH)_2^{4+}$, a mechanism involving only dissociative activation of the strong Fe–O–Fe bond is not particularly attractive. It is reasonable to expect that oxo-bridged dimer breakup follows a pathway involving some assistance due to binding of an entering H_2O molecule. In our proposed mechanism, a symmetrical dihydroxo-bridged complex presumably acts as an unstable intermediate.

$$[(EDTA\text{–}Fe)_2O]^{4-} + H_2O \rightleftharpoons$$

$$[(EDTA)Fe(\overset{H}{O}\overset{O}{H})Fe(EDTA)]^{4-} \rightleftharpoons 2[EDTA\text{–}FeOH]^{2-}$$

The instability of the dihydroxo-bridged complexes in Fe^{III}-EDTA and Fe^{III}-HEDTA systems can be understood because of the expected strain in the bridge of a seven-coordinate structure.

An alternative process for dimer breakup could involve intramolecular assistance from one of the two acetate groups which are likely to be uncoordinated in each Fe^{III}-EDTA dimer. Such a process does not appear consistent with the qualitative observation that the dimer containing HEDTA dissociates at least as fast as $(EDTA\text{-}Fe)_2O^{4-}$. Independent measurements of k_f for both of these dimers by the stopped-flow technique are now in progress.[19]

Acknowledgments. The initial studies involved chronopotentiometric measurements at Columbia University; we thank Professor William Reinmuth and his group for their help in this work. We also thank Dr. Stephen Feldberg of the Brookhaven National Laboratory for supplying the computer working curves required for the kinetic analysis presented in this paper.

(19) J. Earley, private communication.

Kinetics of the Reactions of Bis(glyoximato)cobalt(II) Complexes with Organic Halides[1]

Peter W. Schneider, Patrick F. Phelan, and Jack Halpern

Contribution from the Department of Chemistry, University of Chicago, Chicago, Illinois 60637. *Received August 2, 1968*

Abstract: Various bis(glyoximato)cobalt(II) complexes of the types[2] $Co(DH)_2B$ and $Co(DH)_2B_2$ were found to react quantitatively with benzyl bromide in benzene and acetone solutions to yield $PhCH_2Co(DH)_2B$ and $BrCo(DH)_2B$ according to eq 5 and 6. Evidence is presented that the $Co(DH)_2B_2$ compounds are completely dissociated in solution into $Co(DH)_2B$ and B. All the reactions exhibited second-order kinetics, according to the rate law, $k[Co(DH)_2B][PhCH_2Br]$. At 25°, the value of k for the reaction of pyridinatobis(dimethylgloximato)cobalt(II) in benzene solution is $3.0 \times 10^{-1}\ M^{-1}\ sec^{-1}$. The value of k increases slightly with the basicity of the axial ligand B but is relatively insensitive to variation of the glyoxime ligand. 1-Bromoethylbenzene reacts similarly but at a significantly higher rate. The results are interpreted in terms of a free-radical mechanism, depicted by eq 11 and 12, analogous to that previously proposed for the reactions of pentacyanocobaltate(II) with organic halides. This mechanism involves a rate-determining halogen-atom abstraction by the cobalt(II) complexes.

Considerable interest has been evidenced in recent years in reactions of low-spin complexes of cobalt(I) and cobalt(II) with organic halides to form organocobalt compounds. Such reactions have been described for pentacyanocobaltate(II)[3–5] as well as for cobalt complexes of dimethylglyoxime (cobaloximes),[6–8] and of Schiff bases derived from salicylaldehyde[9] and from acetylacetone.[10] Contributing to the great interest in this subject are the striking parallels, revealed particularly by the work of Schrauzer,[11] between these reactions and the corresponding reactions of the reduced forms of vitamin B_{12}, *i.e.*, vitamin B_{12s} and vitamin B_{12r}.

Two such reactions that have received particular attention and that have been the subjects of kinetic investigations are (i) the reactions of pentacyanocobaltate(II) with a variety of organic halides[3–5] (RX = CH_3I, etc.) according to eq 1

$$2Co(CN)_5^{3-} + RX \longrightarrow RCo(CN)_5^{3-} + XCo(CN)_5^{3-} \quad (1)$$

(ii) the reactions of cobaloximes(I) (*e.g.*, tributylphosphinebis(dimethylglyoximato)cobalt(I), $Co(DMH)_2PBu_3^-$), with organic halides, according to eq 2.

(1) This work was supported in part by the National Science Foundation through a research grant and through a Predoctoral Fellowship Award (to Patrick F. Phelan). Support in part by a Public Health Service Fellowship (No. 1-F2-GM-35,529-01 to Peter W. Schneider) from the Institute of General Medical Science also is gratefully acknowledged.

(2) The following abbreviations are used throughout this paper to designate the various ligands: DH_2 = any glyoxime including one of the following: DMH_2 = dimethylglyoxime, *i.e.*, $HON{=}C(CH_3)C(CH_3){=}NOH$; DPH_2 = diphenylglyoxime; $DMPH_2$ = 4,4′-dimethoxydiphenylglyoxime; $DNPH_2$ = 4,4′-dinitrodiphenylglyoxime. B = any Lewis base serving as an axial ligand including one of the following: PPh_3 = triphenylphosphine; pyr = pyridine; pic = γ-picoline; nic = nicotinamide.

(3) J. Halpern and J. P. Maher, *J. Am. Chem. Soc.*, **86**, 2311 (1964).

(4) J. Halpern and J. P. Maher, *ibid.*, **87**, 5361 (1965).

(5) J. Kwiatek and J. K. Seyler, *J. Organometal. Chem.*, **3**, 421 (1965).

(6) G. N. Schrauzer and J. Kohnle, *Chem. Ber.*, **97**, 3056 (1964).

(7) G. N. Schrauzer and R. J. Windgassen, *J. Am. Chem. Soc.*, **88**, 3738 (1966).

(8) G. N. Schrauzer and R. J. Windgassen, *ibid.*, **89**, 1999 (1967).

(9) G. Costa, G. Mestroni, and G. Pellizer, *J. Organometal. Chem.*, **11**, 333 (1968).

(10) G. Costa and G. Mestroni, *ibid.*, **11**, 325 (1968).

(11) See G. N. Schrauzer, *Accounts Chem. Res.*, **1**, 97 (1968), and references therein.